

Impact of Rearing Conditions and Short-Term Light Exposure on Signaling Performance in *Drosophila* Photoreceptors

Verena Wolfram and Mikko Juusola

Physiological Laboratory, University of Cambridge, Cambridge CB2 3EG, United Kingdom

Submitted 2 March 2004; accepted in final form 12 May 2004

Wolfram, Verena and Mikko Juusola. Impact of rearing conditions and short-term light exposure on signaling performance in *Drosophila* photoreceptors. *J Neurophysiol* 92: 1918–1927, 2004. First published May 19, 2004; 10.1152/jn.00201.2004. The amount of visual information an animal can extract from its environment is ultimately limited by the signaling performance of its photoreceptors. To maximize their performance, photoreceptors must be able to accommodate large changes in input caused by the dynamic properties of the visual environment and the animal's own behavior. This is likely to require a range of adaptation mechanisms operating over multiple time scales. Using intracellular recordings, we investigated the effects of developmental light rearing conditions and the effects of 2 h light or dark exposure prior the experiment on the signaling performance of adult *Drosophila melanogaster* photoreceptors. We show that light-rearing amplifies photoreceptors' voltage responses to light contrast changes by $\geq 20\%$ and accelerates them by 3 ms. We argue that these differences mostly reflect changes in the timing of the early photo-transduction reactions, some of which are persistent. However, being born and nurtured in certain lighting conditions does not set an ultimate limit for the signaling performance of *Drosophila* photoreceptors. Two-hour light exposure prior to the experiment can improve the information capacity of dark-reared photoreceptors close to the values of light-reared photoreceptors by reducing voltage noise. This effect may originate from plastic changes in the utilization of photo-transduction proteins and ion channels.

INTRODUCTION

Neural activity, itself influenced by environmental and genetic variation, is a prerequisite for the correct maturation and refinement of neural circuitry (Desai et al. 2002; Goodman and Shatz 1993; Katz and Shatz 1996; Suster and Bate 2002). Environmental influences continuing throughout adult life cause the structure and function of the nervous system to be adjusted in an experience-dependent manner (Bavelier and Neville 2002; Crair et al. 1998; Knudsen and Brainard 1991; Mooney 1999; Palleroni and Hauser 2003). Although the detailed mechanisms underlying such experience-dependent plasticity remain unclear, they include alterations in strength of synaptic connections between cells by Hebbian (Bear and Malenka 1994) or homeostatic (Davis and Goodman 1998a,b; Turrigiano 1999) mechanisms and reshaping of neural circuits (Bavelier and Neville 2002; Brainard and Doupe 2002).

Experience-dependent neural plasticity has been extensively studied in vertebrate cortical circuits (Bavelier and Neville 2002; Brainard and Doupe 2002; Mooney 1999; Turrigiano 1999), including the visual cortex (Katz and Shatz 1996), where the development of ocular dominance columns is influ-

enced by sensory experience (Hubel and Wiesel 1970; Hubel et al. 1977). Invertebrate visual centers also undergo experience-dependent plasticity (Deimel and Kral 1992; Hertel 1982, 1983; Kral and Meinertzhagen 1989; Meinertzhagen 1989; Mimura 1986). For example, Barth (1997) and Barth et al. (1997) showed an effect of environmental conditions on structure in the visual processing centers of an insect brain: changing the duration of light exposure during development altered the size and shape of the lamina, mushroom bodies, and central complex.

Most studies of experience-dependent plasticity have focused on synaptic connections between interneurons downstream of sensory receptors, but experience-dependent changes may also happen within sensory receptors. In recent years, *Drosophila* photoreceptor cells have become one of the best-studied model systems for receptor-mediated Ca^{2+} entry and G-protein signaling (Hardie 1991b; Hardie and Raghu 2001). *Drosophila* photoreceptors can respond to light changes with great rapidity within an intensity range that spans over seven orders of magnitude (Juusola and Hardie 2001a). Occurring at different stages of optical, chemical, and electrical signal processing and at different time scales, adaptation both prevents photoreceptors' responses from saturating and improves their temporal resolution (Hardie and Raghu 2001; Juusola and Hardie 2001a).

Early electrophysiological studies of insect photoreceptors describe rapid adaptation mechanisms (Laughlin and Hardie 1978) by which sensitivity decreases and response speed increases in bright light (Laughlin 1989). These changes are reversible and are observed at the level of the "bump," the discrete fluctuation of light current [i.e., the current flowing through the light-dependent ion channels, transient receptor potential (TRP), and like transient receptor potential (TRPL)] triggered by a single photon (cf. Hardie and Raghu 2001; Henderson et al. 2000; Juusola et al. 1994; Wong et al. 1980). The responses are further shaped by the activation of voltage-dependent K^{+} -channels (Weckström and Laughlin 1995; Weckström et al. 1991). More recently, reversible light-regulated translocation of signaling molecules to and from rhabdomere, the light sensitive part of the photoreceptor, has been proposed to contribute to light adaptation. Within 2 h of light exposure, $\text{Gq}\alpha$ and TRPL cation channels are shuttled out of the rhabdomere, while arrestin (Arr2) gets enriched in the rhabdomere (Bähner et al. 2002; Kiselev et al. 2000; Kosloff et al. 2003; Lee et al. 2003). In addition, complementary molecular dynamics in phototransduction cascade, membrane filter-

Address for reprint requests and other correspondence: M. Juusola, Physiological Lab., Univ. of Cambridge, Cambridge CB2 3EG, UK (E-mail: mj216@cam.ac.uk).

The costs of publication of this article were defrayed in part by the payment of page charges. The article must therefore be hereby marked "advertisement" in accordance with 18 U.S.C. Section 1734 solely to indicate this fact.

ing, or adaptation are likely to occur. However, without electrophysiological data, one cannot bind these plastic, or long-term reversible, changes to the changes in the photoreceptors' signaling performance. Using intracellular recordings from adult *Drosophila* photoreceptors, we now show that 12:12 h light:dark rearing amplifies and accelerates their responses to light contrast changes and decreases their membrane resistance in comparison to dark-rearing. Unlike the previous findings, these changes are persistent since a 2 h dark exposure is not sufficient to reverse the effects. Nevertheless, after 2 h of light exposure, photoreceptors show additional plastic changes in their signaling that improve their information capacity.

METHODS

Fly stocks and rearing scheme

Drosophila melanogaster flies of the red-eyed wild-type stock Oregon Red were used in all experiments. Flies were reared for several generations on standard *Drosophila* medium in a 19°C incubator. Flies lived in light-proofed boxes (12.5 × 12.5 × 9 cm) under two light conditions: in a 12 h light/12 h dark cycle and in constant darkness, referred to as light-reared (LR) and dark-reared (DR), respectively. The light-rearing box was painted white inside to enhance light reflection and was equipped with an array of six white LEDs (SMD, 320 mcd with viewing angle 105°, Marl Optosource) run by a 12 V battery to generate the light:dark cycle. The maximum light scatter inside the box was 100 cd/m². Food for DR flies was changed under dim red light to minimize the probability of photon capture by rhodopsin.

All experiments were carried out in the hours of late morning and early afternoon. In the morning, 2 h prior to each experiment, specimens from each LR and DR population were exposed to either darkness (DE) or light (LE), thereby generating four different fly regimens: LRLE, LRDE, DRLE, and DRDE, all having ancestry in the same initial population.

Preparation and electrophysiology

Flies (2–10 days old) were mounted in a conical holder made from copper and ceramic. To prevent visual artifacts caused by head or body movements, we applied beeswax to the thorax, proboscis, and one eye (Juusola and Hardie 2001a). A small window, size of few ommatidia, was cut in the dorsal cornea for entry of a recording microelectrode and sealed with Vaseline. LRDE and DRDE flies were prepared under red light. A blunt reference electrode filled with fly Ringer solution, containing (in mM) 120 NaCl, 5 KCl, 10 TES, 1.5 CaCl₂, and 4 MgCl₂, was placed in the head capsule close to the ocelli. The temperature of the flies was maintained at 25°C by a feedback-regulated Peltier-element placed beneath the holder (Juusola and Hardie 2001a).

Intracellular recordings were carried out from green-sensitive R1-6 photoreceptor cells with sharp quartz microelectrodes (Sutter Instrument) filled with 3 M KCl and with resistances between 100 and 220 MΩ. The voltage and current signals were amplified by a switch-clamp amplifier (SEC-10L, NPI Electronic) using switching frequencies of ~15 kHz and low-pass filtered at 500 Hz (elliptic) in current-clamp mode. The photoreceptors were selected for analysis only if their resting potential in darkness was less than -50 mV and the magnitude of the responses to a saturating light step was ≥40 mV. To accomplish the required recordings, the experiments from a single photoreceptor lasted typically 30 min.

Light stimulation and data analysis

Photoreceptors were stimulated with light from a small field (5° as seen by the fly) generated by a high-intensity green LED with a peak

wavelength of 525 nm (Marl Optosource) that was driven by a custom-built driver. Background intensity was attenuated by combinations of seven neutral density filters, each reducing the light intensity by one-half a log-unit, placed between the light source and the eye.

Two types of light stimulus were used throughout the experiment: band-limited Gaussian white noise contrast (WNC; with cut-off at 300 Hz) lasting 10 s and a 700 ms saturating light pulse. The Gaussian white noise stimulus was superimposed on a constant light background (BG), and its intensity values were converted to contrast values, $c(t)$ [$c(t) = \Delta I/I$, where ΔI is the intensity change, and I is the mean intensity over time]. The characteristic contrast of WNC was 0.32, defined by dividing the SD of the contrast values by the unit mean (Juusola et al. 1994). Prior to recording, photoreceptors were adapted for 30 s to a chosen light BG. This time was considered sufficient for the photoreceptors to adapt to a steady-state potential that remained virtually unchanged during the actual WNC stimulation. The light BGs covered 3.5 log units with minimum intensity of ~950 photons/s (BG-3.5) and maximum intensity, I_0 , of $\sim 3 \times 10^6$ photons/s (BG0). Details of calibration procedure are given in Juusola and Hardie (2001a). In a typical experiment, the photoreceptor was first studied at BG-3.5 before systematically proceeding to brighter BGs. At each BG, the stimulation lasted $10 \times (10 + 1s) = 110$ s (repetitions × [stimulus duration + delay]). Light stimuli were delivered at 1 kHz, and voltage responses were sampled at 1 kHz. Stimulus generation, data acquisition, and signal analysis were performed by a MATLAB interface, BIOSYST (copyright M. Juusola 1997–2002) with a custom-written control for National Instrument boards (copyright MATDAQ, H.P.C. Robinson 1997–2001).

WNC was delivered to the photoreceptor 10 times, each presentation evoking slightly different voltage responses, $r(t)$. Averaging these responses gave the noise-reduced photoreceptor voltage signal, $s(t)$ (Juusola et al. 1994; Kouvalainen et al. 1994). To obtain the noise, $n(t)$, of each individual response, the signal, $s(t)$, was subtracted from each response, $r(t)$. As the stimulation was given after a photoreceptor had reached a steady-state potential, the noise traces did not show any obvious adaptation trends.

To avoid a possible bias of the noise estimates by the low number of samples, the noise was also calculated using a method that did not allow signal and noise to be correlated (Juusola and French 1997). In brief, when an experiment consisted of 10 trials, 9 of the trials were used to compute $s(t)$ and the other to compute $n(t)$. Repeating this for each possible set of nine responses gave 10 uncorrelated noise traces. In accordance with Juusola and Hardie (2001a), these two methods gave similar noise estimates with very low variance. As stated earlier by Kouvalainen et al. (1994), errors due to residual noise in $s(t)$ are small and proportional to (noise power)/sqrt(n), where n is 10.

$s(t)$ and $n(t)$ were segmented into 50% overlapping stretches (each 1,024 points long) and windowed with a Blackman-Harris four-term window before their corresponding spectra, $S(f)$ and $N(f)$, were calculated with a fast Fourier transform (FFT) algorithm, yielding 18 and 180 samples, respectively. Signal and noise power spectra, $\langle S(f) \rangle^2$ and $\langle N(f) \rangle^2$, respectively, were calculated as real-valued functions, where $\|$ denotes the absolute value and $\langle \rangle$ denotes the average over the different stretches of the signal and noise data (cf. Juusola and Hardie 2001a). In the same way, the stimulus presentations $c(t)$ yielded the power spectra $\langle C(f) \rangle^2$ used for calculating the impulse response (see following paragraph). The large number of spectral samples made the error in the mean power spectral estimate small (Bendat and Piersol 1986). Our tests where random noise was added on a band-passed signal waveform indicated that, for data of equal size (10 traces lasting 10 s or 10,000 points), the mean square error in the power spectral estimate is ~15% over frequencies from 1 to 200 Hz. This estimate was extrapolated after calculating the power spectra from 10 and 1,000 traces (see also Juusola and de Polavieja 2003).

The signal-to-noise ratio in the frequency domain, $SNR(f)$ was obtained by dividing the signal power spectrum, $|S(f)|^2$, by the corresponding noise power spectrum, $|N(f)|^2$ (Kouvalainen et al. 1994). After 30 s of adaptation to the given light BG, photoreceptors produce approximately linear responses to the WNC (Juusola and Hardie 2001a). This is judged by their coherence functions (for analysis, see Bendat and Piersol 1986) that typically approach unity (values > 0.9) over frequencies from 1 to 50 Hz (data not shown; cf. Juusola and Hardie 2001a). The high degree of linearity, together with approximately Gaussian signal and noise distributions, justifies the calculation of information capacity, C , from $SNR(f)$ by Shannon's formula (Shannon 1948)

$$C = \int_0^{\infty} \log_2(SNR(f) + 1) df \quad (1)$$

The information capacity is a measure of the number of states a signaling system can transmit per unit time. The dimension of the information capacity is bits/s. Owing to the unreliability of the signal at frequencies > 200 Hz, this was set to be the upper limit of the integral instead of ∞ (Juusola and Hardie 2001a). Since $s(t)$ and $n(t)$ are not always purely Gaussian, but sometimes slightly skewed (cf. Juusola and Hardie 2001a), the information capacity estimates determined here can only be considered as approximations of the true information capacity (Juusola and French 1997; Shannon 1948). The information capacity estimates are further influenced by the fact that the photoreceptor noise power includes the electrode noise. This causes a slight underestimation of the true information capacity values. Additionally, any systematic trends in the thermal membrane noise (as imbedded in the measure of voltage noise) between different photoreceptors could potentially bias the differences in the information capacity estimates between the rearing groups (Juusola and Hardie 2001b). However, this is considered unlikely since the eye temperature (25°C) varied $< 1^\circ\text{C}$ during each experiment (cf. Juusola and Hardie 2001a), and the membrane capacitance, as a measure of the membrane area that contributes to such noise, was similar for the photoreceptors of different rearing groups (cf. Fig. 3C).

The final estimates of $\langle |S(f)|^2 \rangle$ and $\langle |N(f)|^2 \rangle$ and C for each test regimen we present in Figs. 4 and 5, respectively, are the means of the corresponding functions from all the successful experiments with the data coming from different flies. Any errors in these unbiased estimates, brought by the errors in power spectra of individual recordings ($\sim 15\%$), diminished progressively as the number of photoreceptors used for the analysis increased (being ≥ 5).

The linear filter properties of the photoreceptor are defined in the time domain by the impulse response, $k_v(t)$, calculated from the spectral estimates of the input (WNC) and output (signal) (French et al. 1972; Marmarelis and Marmarelis 1978; for details, see Juusola and Hardie 2001a). Impulse responses were fitted with the log-normal function (Payne and Howard 1981)

$$k_v(t) = A \times \exp\left\{-\frac{[\log(t/t_p)]^2}{2\sigma^2}\right\} \quad (2)$$

where A is the amplitude of the impulse response, t is time after flash delivery, t_p is the time-to-peak of the impulse response, and σ is the width factor that determines the ratio between impulse response duration and time-to-peak. A , t_p , and the times of half-maximal amplitude t_1 and t_2 were analyzed. The half-width, h_w , thus corresponds to the difference between t_2 and t_1 , half-rise time corresponds to $t_p - t_1$, and half-decay time corresponds to $t_2 - t_p$ (Fig. 1A).

Voltage responses to the 700 ms light step were analyzed with respect to the peak, trough, and plateau phase (Fig. 7), as well as the occurrence of oscillations. To analyze the oscillations, the voltage response was segmented into half-overlapping windows of 128 data points (corresponding to 128 ms), allowing detection of frequencies as

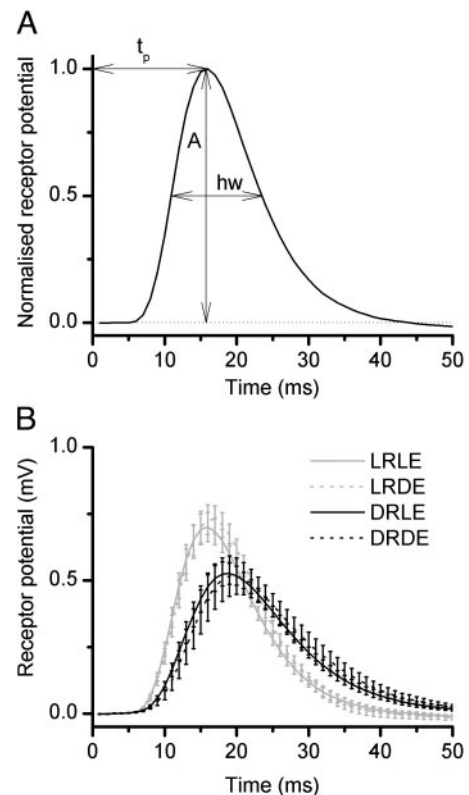


FIG. 1. Time course of photoreceptor impulse responses is affected by rearing conditions. *A*: impulse responses, calculated from the responses to white noise contrast stimuli, were fitted with lognormal functions; indicated are the time-to-peak (t_p), amplitude (A), and times at which one-half the amplitude is reached (t_1 and t_2). The half-width (h_w) is the difference between t_2 and t_1 , half-rise time is the difference between t_p and t_1 , and half-decay time is the difference between t_2 and t_p . *B*: impulse responses of light-reared light-exposed (LRLE; $n = 15$), light-reared dark-exposed (LRDE; $n = 6$), dark-reared light-exposed (DRLE; $n = 11$), and dark-reared dark-exposed (DRDE; $n = 5$) photoreceptors at background (BG)-0.5. Impulse responses are calculated per unit contrast. Means and SE are plotted.

low as 8 Hz. For each window, a power spectrum was calculated using an FFT. The major frequency components of each window were plotted against time to obtain a dynamic spectrum.

Current stimulation

Depolarizing and hyperpolarizing current steps of maximum amplitude ± 0.2 nA were injected into photoreceptors in darkness in current-clamp mode. The smallest current step (-0.02 nA) was used to calculate the membrane resistance, R_m , and the effective capacitance, C_m . To calculate the effective capacitance, we adapted a method originally used in voltage-clamped striated muscles (Adrian and Almers 1974; Schneider and Chandler 1976). This method is robust against voltage noise, not biased by curve fitting, and well suited for cells that have additional membrane foldings (such as rhabdomere).

An injection of a small negative step current, I_{∞} , into a *Drosophila* photoreceptor in darkness causes an exponential voltage change that reaches a steady-state value, V_{\max} , before the end of the step (Fig. 3A), characteristic of a passive membrane. This voltage waveform, $V = I_{\infty} R_m [1 - \exp(-t/R_m C_m)]$, allows us to determine the effective capacitance, C_m . Dividing V by the measured resistance, $R_m = V_{\max}/I_{\infty}$, gives us the current flowing through the purely resistive pathways: $I_{\text{res}} = I_{\infty} [1 - \exp(-t/R_m C_m)]$. The transient capacitive current is: $I_{\text{cap}} = I_{\infty} - I_{\text{res}} = I_{\infty} \exp(-t/R_m C_m)$. Integrating over I_{cap} gives the charge, Q , stored in the membrane. C_m is then Q/V_{\max} .

Statistical analysis

Results of each test regimen are expressed as means \pm SE. Statistical differences between means were analyzed using two-way ANOVA. Both rearing and exposure were kept as fixed factors. We tested for similarities of the mean at the rearing level and the exposure level by taking interaction into account. The ANOVA was performed at seven background light intensities (BG-3 to BG0). We postexamined the results using the Bonferroni test. All statistics were performed in Microcal Origin 7SR2.

RESULTS

Drosophila photoreceptors are complex dynamic systems whose voltage responses to light show different degrees of nonlinearities depending on the visual stimulus. We used band-limited Gaussian WNC stimulation to have an adequate control over their response dynamics and to minimize the nonlinear components of the voltage output (Juusola et al. 1994; Juusola and Hardie 2001a; Spekreijse and Oostings 1970; Spekreijse and van der Tweel 1965). WNC covers the majority of stimulus frequencies that may be encountered by flies in vivo (note that spectra of natural images experienced by moving animals tend to approximate $1/f$, with f as stimulus frequency; cf. Juusola and de Polavieja 2003; van Hateren 1992), thus justifying our approach to quantify the photoreceptor's ability to encode dynamic light changes. As the variance of WNC is constant at different mean adapting BGs, we can make fair comparisons about the effects of rearing light conditions and light/dark exposure on photoreceptor signaling performance and adaptability.

Impulse responses

Impulse responses, k_v , calculated from the photoreceptor responses to WNC not only define the filtering in time domain (Fig. 1A) but also closely resemble the actual voltage responses of light-adapted photoreceptors to a light flash (Juusola 1993; Juusola et al. 1994). The amplification and speed of the impulse responses were characterized by their peak amplitude (A) and kinetic (or time-characterized) parameters: time-to-peak (t_p), half-width ($t_w = t_2 - t_1$), half-rise time ($t_r = t_p - t_1$), and half-decay time ($t_d = t_p - t_1$; Fig. 1A), respectively. Figures 1B and 2 show that rearing conditions exerted major effects on these parameters, whereas the exposure conditions contribute relatively little. Figure 1B depicts impulse responses for the four test regimens at BG-0.5. Here the impulse responses of LR flies (LRLE, $n = 15$ and LRDE, $n = 6$) are 26% larger (A; $P \sim 0.004$, for rearing; Table 1) and 20% faster (t_p ; $P < 0.001$, for rearing) than those of DR flies (DRLE, $n = 11$ and DRDE, $n = 5$). Figure 2, on the other hand, shows the general statistics of the maximum amplitudes and kinetic parameters at different BGs for the four test regimens.

AMPLIFICATION. The amplitude of the linear impulse responses (Fig. 2A) gives a practical measure of the photoreceptor sensitivity to light contrast changes, often called contrast gain. All four regimens show increase in the contrast gain with brightening BG, the degree of which is influenced by the rearing conditions. The impulse response amplitudes of LR photoreceptors are generally larger than those of DR photoreceptors ($\sim 25\%$) except at the very dim BGs, where they are indistinguishable (Fig. 2A; Table 1). The exposure conditions,

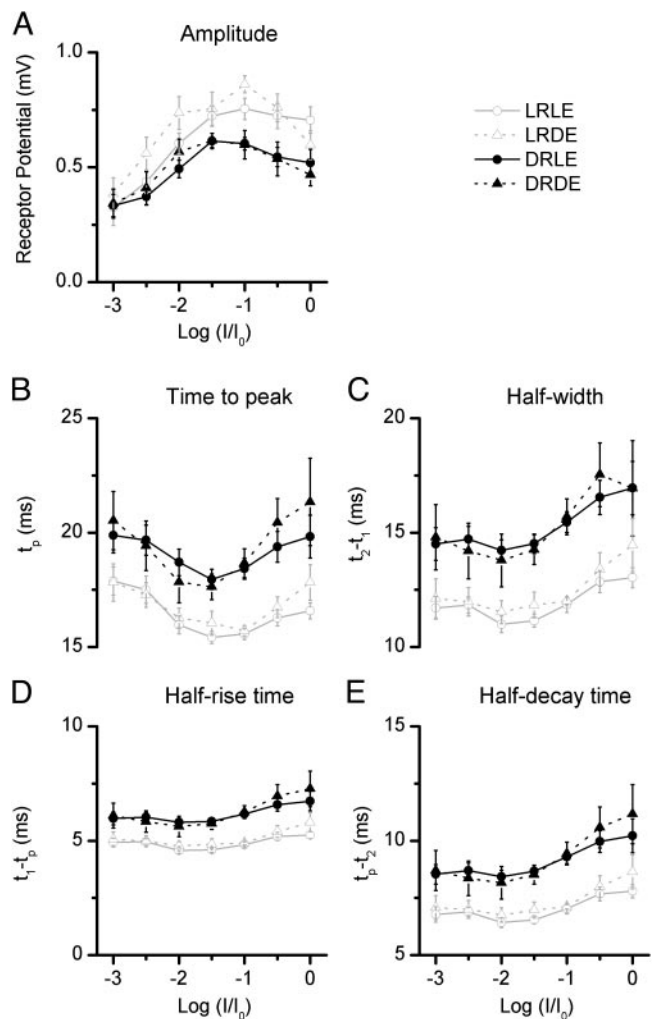


FIG. 2. Light-rearing has a major effect on the maximum amplitude (A) and the kinetic parameters (B–E) of impulse responses. B: time-to-peak, t_p . C: half-width. D: half-rise time. E: half-decay time over the tested light BG range. Exposure introduces slight differences in the kinetic parameters at bright BGs. Light reared flies have higher contrast gains or larger amplitudes (A) than dark-reared flies. Dark-rearing slows down the photoreceptor responses (B–E). All data shows means \pm SE, where n is the same as in Fig. 1.

on the other hand, did not produce significant differences on the contrast gain (Fig. 2A).

SPEED. LR accelerates the overall time course of the responses: time-to-peak of LR photoreceptors is reached 3 ms earlier and half-width is 3 ms less than those of DR photoreceptors at all BGs (Fig. 2, B and C, respectively). In all test regimens, time-to-peak and half-width first decrease with brightening light until BG-1.5 and thereafter increase at the brighter BGs (Fig. 2, B and C; cf. also Juusola 1993), owing to saturation. However, exposure conditions (LRLE, DRLE vs. LRDE, DRDE) introduce slight variations in these U-shaped trends (Fig. 2, B and C). For example, at bright BGs, impulse responses of DE photoreceptors peak later (Fig. 2B) and are broader than those of LE photoreceptors (Fig. 2C).

A general feature of impulse responses is their abrupt rising and slightly slower decaying phase (Fig. 1A). Because there are a number of ways for the phototransduction reactions involved in the timing and shaping of the elementary responses, or bumps, to influence these dynamics separately (Henderson et

TABLE 1. Statistics of photoreceptor impulse response amplitudes for the test regimens

	BG-3	BG-2.5	BG-2	BG-1.5	BG-1	BG-0.5	BG 0
P value two-way ANOVA for rearing	0.803	0.069	0.018	0.031	<0.001	0.004	0.067
P value two-way ANOVA for exposure	0.61	0.171	0.074	0.749	0.339	0.837	0.334
Significant at 0.05 level Bonferroni test for rearing	No	No	Yes	Yes	Yes	Yes	Yes
Significant at 0.05 level Bonferroni test for exposure	No	No	Yes	No	No	No	No

al. 2000; Juusola and Hardie 2001a,b; Wong et al. 1980), we investigated whether the changes in the half-width reflected selective changes either in the rising or decaying phase. Since dark rearing slows down both the half-rise and half-decay time in equal proportions (by 20%; Fig. 2, C and D), the phototransduction reactions must be tightly coupled and scalable processes (cf. Juusola and Hardie 2001a,b).

Effective capacitance and resistance of the photoreceptor membrane

Photoreceptor voltage responses to light stimulation are produced by the light current, resulting from the phototransduction cascade, and filtering of the light current by the cell membrane. The observed changes in the voltage response could result from variations in either of these processes or in both. To find out if the four test regimens had caused any structural changes in the cell membranes of the photoreceptors, we investigated their filtering properties in the darkness, where this estimation is the most accurate (Juusola and Weckström 1993; Weckström et al. 1991).

Figure 3A depicts typical voltage traces of LRLE and DRLE photoreceptors subjected to hyperpolarizing and depolarizing current steps of increasing amplitude, maximum of 0.2 nA. The recordings showed strong, time-dependent, outward rectification, owing to the progressive activation of voltage-sensitive potassium channels from the resting potential onward (Hardie 1991a). Depolarizing pulses elicited voltage responses with approximately square-wave profiles that showed an early peak followed by slower charging. This behavior, caused by the shifted activation and inactivation profiles of *Shaker* channels, selectively amplified slow depolarizing signals (Juusola et al. 2003; Niven et al. 2003). In contrast, the responses to hyperpolarizing pulses were much slower, showing characteristic resistor-capacitor charging. We determined membrane resistance, R_m , and effective capacitance, C_m , from the response to the smallest hyperpolarizing pulse (-0.02 nA) using a step transient integration method (Adrian and Almers 1974) (see METHODS). Although effective capacitances of photoreceptors within the four test regimens were statistically indistinguishable (Fig. 3B), LR photoreceptors had smaller membrane resistances (Fig. 3B) and time constants (Table 2) than DR photoreceptors. Juusola and Hardie (2001a,b) showed that, although the cell membrane provided faster signaling with brightening BGs and was never limiting the speed of the phototransduction cascade, the membranes that low-passed most in darkness frequently also had the lowest cut-off in bright BGs. Thus membranes of LR photoreceptors are likely to provide a broader channel bandwidth with higher cut-off frequencies during light adaptation than membranes of DR photoreceptors (Table 2).

Signal and noise dynamics and information capacity

Figure 4 compares the mean signal (*left*) and noise (*right*) power spectra of photoreceptors from the four regimens at four

different light BGs (BG0, BG-1, BG-2, and BG-3). In all cases, brightening the BG increased the signal power and broadened the frequency range until saturation at BG-1 (Fig. 4; *left*; cf. Juusola and Hardie 2001a). Consistent with their faster impulse responses and membrane properties, signals of LR photoreceptors had significantly more power at high frequencies, ≥ 50 Hz, than DR photoreceptors (Fig. 4; *left*). Light exposure, on the other hand, had a limited effect on the signal bandwidth, yet it appeared to give some protection against the collapse of the signal power at the brightest BG (Fig. 4; *left*; cf. BG-1 to BG0).

The noise power fell with increasing BG (Fig. 4; *right*; cf. Juusola and Hardie 2001a) for all regimens. Together with the simultaneously increasing signal power, this improved the signal-to-noise ratio, $SNR(f)$, leading to higher information capacities (Fig. 5B). Light exposure has a major impact by decreasing the noisiness of the voltage responses at all BGs. Since LE photoreceptors were less noisy than DE photoreceptors but had similar signals, LE photoreceptors had a higher signal-to-noise ratio and information over the response bandwidth than DE photoreceptors (Fig. 5A). Consequently, light exposure increased the information capacity by 20–30% at brighter BGs (Fig. 5B; cf. LRLE to LRDE and DRLE to DRDE).

Photoreceptors appeared to utilize two different coding strategies that complement the adjusted filtering properties of the

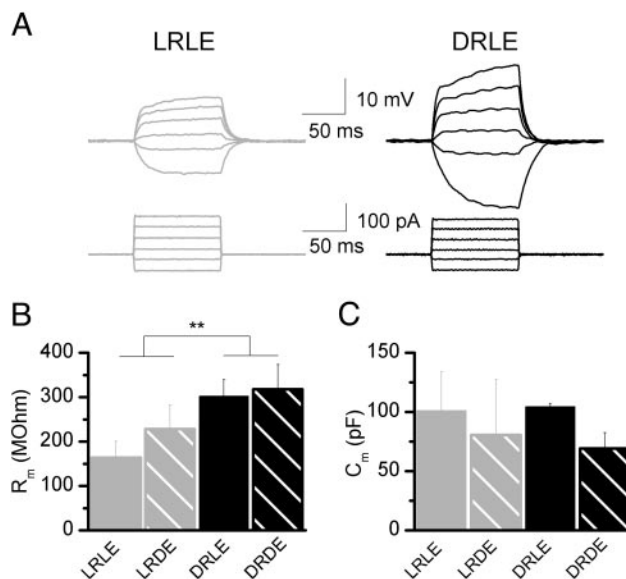


FIG. 3. Rearing conditions influence photoreceptor voltage responses to injected current steps by changing the membrane resistance. A: typical current step responses of LRLE and DRLE photoreceptors. Photoreceptors are stimulated with hyper- and depolarizing current steps of maximum amplitude of 0.2 nA. The smallest hyperpolarizing current step was used to calculate the membrane resistance, R_m (B) and the effective capacitance, C_m (C). B: membrane resistance of LR photoreceptors is significantly less than membrane resistance of DR photoreceptors (2-way ANOVA for rearing: $**P < 0.03$). C: effective capacitance for the photoreceptors of the 4 test regimens.

TABLE 2. *Effective photoreceptor capacitance and membrane resistance for the test regimens*

	LRLE	LRDE	DRLE	DRDE	Statistics
No of cells	4	3	5	3	
C_m (pF)	101 ± 33	81 ± 47	105 ± 3	69 ± 13	Two-way ANOVA Rearing $P \sim 0.8$ Exposure $P \sim 0.3$
R_m (M Ω)	164 ± 37	228 ± 54	302 ± 37	318 ± 55	Two-way ANOVA Rearing $P < 0.03$ Exposure $P \sim 0.3$
τ_m (ms)	13.2 ± 2.7	14.8 ± 5.7	31.8 ± 4.2	20.6 ± 0.9	Two-way ANOVA Rearing $P = 0.01$ Exposure $P = 0.25$

Values are means ± SD.

photoreceptor membrane (cf. Fig. 3A). Where LRLE photoreceptors could transmit faster signals than DRLE photoreceptors, DRLE photoreceptors compensated for this loss by having more reliable signaling [higher $SNR(f)$] over their narrower bandwidth (cf. Fig. 5, A and B). The outcome was a relatively

similar information capacity for both regimens. Accordingly, the lower voltage noise of DRDE photoreceptors helped them to approach the information capacities of LRDE photoreceptors (cf. Fig. 5, A and B).

Steady-state membrane potential

Prior to contrast stimulation, photoreceptors were adapted to given light BGs, whereby their depolarization gradually approached a steady-state potential, on which the contrast-induced responses were superimposed. In all test regimens, the steady-state depolarization shows a sigmoidal dependency on the adapting BG intensity and was fitted with the self-shunting model [$V = V_{max}I^p/(I^p + I_{50}^p)$; cf. Laughlin 1989; Fig. 6]. Thus the steady-state potential represents a static nonlinearity in phototransduction. Photoreceptors of both DR regimens (DRLE and DRDE) as well as the LRDE ones had similar steady-state potentials at all BGs, whereas photoreceptors of the LRLE regimen showed a noticeable reduction in their steady-state potential following light exposure.

Voltage responses to bright pulses

We next analyzed the behavior of the photoreceptor responses during the rapid nonlinear adaptation phase leading to the steady-state potential. All photoreceptors from the four test regimens responded to a long bright pulse with waveforms

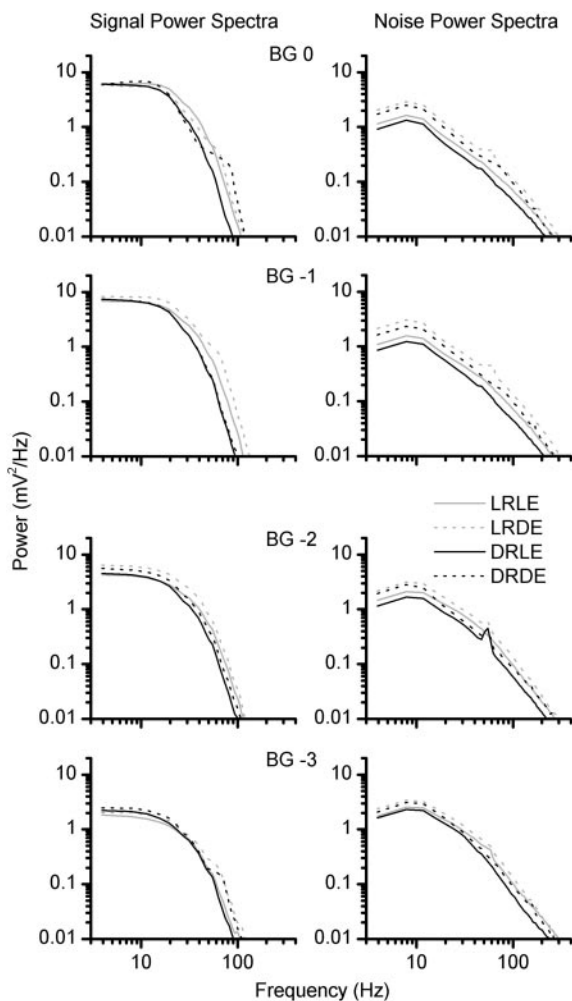


FIG. 4. Mean signal power spectra (*left*) and corresponding mean noise power spectra (*right*) for the photoreceptors of the test regimens at 4 light BGs (from dim BG-3 to bright BG0). LR increases the signaling bandwidth of photoreceptors. Light exposure helps to prevent voltage responses from collapsing at brighter BGs. All photoreceptors show reduced noise power at brighter light BGs. LR both amplifies and broadens the signal power, while light exposure reduces noise. Traces show the mean, calculated from individual experiments. Number of cells is as in Fig. 1.

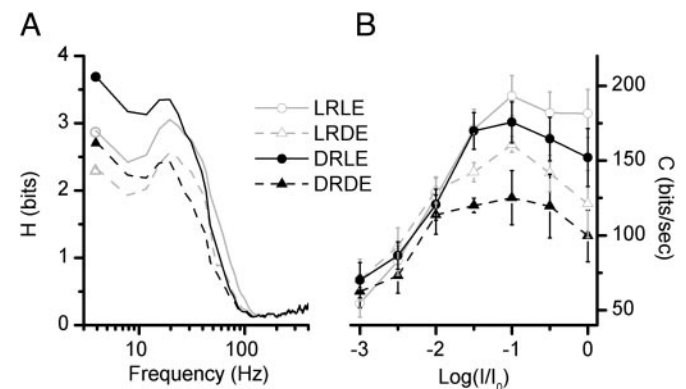


FIG. 5. Frequency distribution of information and information capacity of photoreceptors differ between the 4 test regimens. A: frequency distribution of visual information (in bits), $H = \log_2[SNR(f) + 1]$, in the photoreceptors' voltage responses at BG-0.5 (LRLE, $n = 12$; LRDE, $n = 6$; DRLE, $n = 11$; DRDE, $n = 5$). B: information capacity of the photoreceptors at 7 light BGs. LRLE and DRLE photoreceptors show relatively similar information capacities at all BGs owing to 2 different coding strategies.

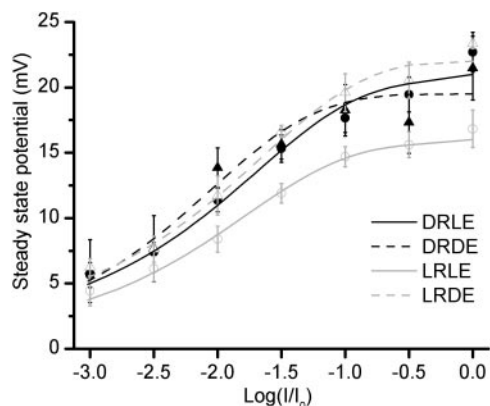


FIG. 6. LRLE photoreceptors have lower steady-state potentials at all BG light intensities. Photoreceptors adapt in response to constant light stimulation, gradually reaching steady-state membrane potentials. Steady-state potentials of the photoreceptors from the 4 test regimens 30 s after the onset of light are plotted as a function of BG light intensities; 0 mV is the dark resting potential. Curves are fitted with the self-shunting model [$V = V_{\max} \times I^n / (I^n + I_{50}^n)$]; V_{\max} is the maximum steady-state potential reached at BG0, I_{50} is the BG intensity that induces half-maximum steady-state depolarization, and n is an empirical exponent. Means and SE are shown.

consisting of three successive stages: the peak, a trough, and a plateau component (Fig. 7, A and B).

In all four test regimens, individual photoreceptor responses to bright light pulses often showed oscillations on their plateau phase (Table 3; Fig. 7, A and B), with frequencies changing in a time-dependent manner. This is highlighted in Fig. 7, C and D, which show the dynamic spectra of LRLE and DRLE photoreceptors, while Table 3 summarizes details of the oscillations for the regimens.

The characteristics and incidence of oscillations depended mainly on rearing conditions. Oscillations occurred more often in photoreceptors of DR flies as opposed to LR flies. In both regimens, the oscillations had similar initial frequencies (90–100 Hz) before slowing down and decaying. Since the oscillations lasted longer in the DR photoreceptors (often until the light was switched off), their final frequencies (50 Hz) were less than those of LR photoreceptors that decayed at about 80 Hz (Fig. 7C; Table 3). Higher order harmonics could be detected in the voltage responses of both LR and DR photoreceptors that were exposed to light (LRLE, DRLE), but not in the voltage responses of photoreceptors that were exposed to darkness. However, DRLE photoreceptors exhibited harmonics more frequently (5/7) than LRLE photoreceptors (2/6; Table 3; Fig. 7D).

DISCUSSION

We investigated how light history affected the ability of *Drosophila* photoreceptors to respond to dynamic contrast stimulus (WNC) at different light intensity levels (BGs). For this, we used both dark and light rearing conditions in combination with 2 h light or dark exposure prior the experiments. We employed an approach that allowed long-lasting stable intracellular recordings from in vivo photoreceptors, giving an accurate and general electrophysiological description of both the phototransduction reactions and the membrane properties in the presence of surrounding cellular structures. Our results show that the signaling performance of *Drosophila* photoreceptors is tuned on different time scales. 1) Rearing conditions

adjust the slow processes that set the amplification and speed of photoreceptor voltage responses. 2) The light or dark exposure can modulate the fast processes that regulate the sensitivity, and thus the precision of the responses, at different BGs. 3) Voltage responses also display fast oscillations during continuous light. We will now discuss the possible molecular mechanisms and coding strategies behind these findings and compare the photoreceptor plasticity to plasticity in higher-order visual centers.

How do photoreceptor cells adjust to rearing light conditions?

The simplest hypothesis would allow light-rearing to alter either the phototransduction cascade's or membrane's filtering function alone. Neither our data (Figs. 3 and 4) nor the data processing inequality (cf. Cover and Thomas 1991) supports this hypothesis. Adjustments of phototransduction gain or membrane filtering alone cannot improve the information capacity of a photoreceptor, as either would, at best, affect signal and noise equally. Instead, the higher information capacity of LRLE photoreceptors (Fig. 5B) must reflect *increased* information capture, requiring improvements in their processing speed, efficiency, or structure over the other photoreceptors. LRLE photoreceptors could have 1) faster or more precisely timed single photon responses, or bumps, 2) less variable bumps (owing to any physical change that reduces photoreceptors' voltage noise; cf. Shannon 1948), or 3) more light-capturing phototransduction units, possibly microvilli (Hamdorf 1979; Howard et al. 1987; Juusola and Hardie 2001a). The

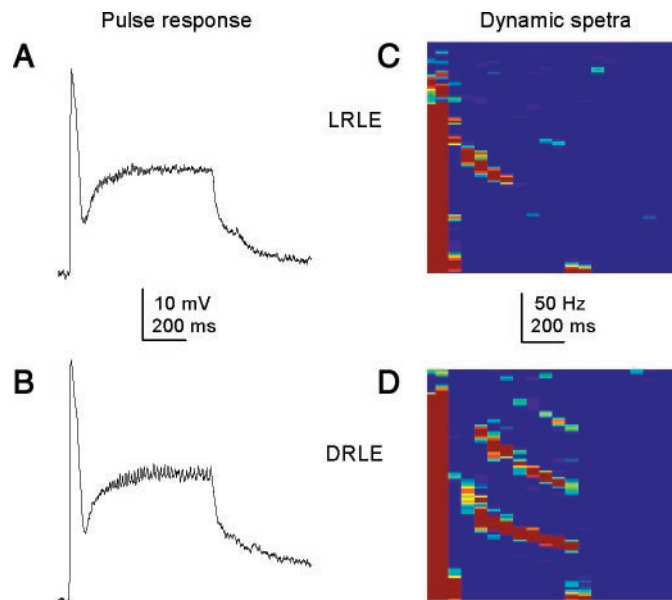


FIG. 7. Photoreceptors exhibit oscillations superimposed onto their voltage responses when stimulated with a bright saturating light pulse lasting 700 ms. A and B: photoreceptor voltage responses of LRLE and DRLE flies, respectively. Both photoreceptors show oscillation with decaying frequency. C and D: dynamic spectra of the same photoreceptor voltage responses as depicted in A and B. Fourier spectra are calculated for half-overlapping windows of 128 data points or ms. Frequency components of each window are plotted vs. the time axis. Peak of the response causes an initial high frequency. However, while the response is reaching the plateau phase, frequency components of 100–50 Hz are observed. Response of the LRLE photoreceptor shows only 1 harmonic, whereas the DRLE photoreceptor shows higher-order harmonics. Intense red color indicates high power.

TABLE 3. Features of oscillations in photoreceptor voltage responses for the four test regimens

	LRLE	LRDE	DRLE	DRDE
Number of cells showing oscillations	6/27 (22%)	1/10 (10%)	7/17 (41%)	6/11 (54%)
Frequency (Hz) at the beginning	100 ± 10	100	90 ± 3	90 ± 10
Frequency (Hz) at the end	75 ± 5	80	55 ± 3	55 ± 5
Disappearance of oscillation	Yes (after 300 ms)	Yes (after 200 ms)	No	No
Harmonics	2/6	No	5/7	No

Values are means ± SD.

latter is true in blowfly (*Calliphora vicina*) photoreceptors, whose photosensitive part, the rhabdomere, contain three times more microvilli, ~90,000, than *Drosophila* (Hardie 1985) and have about three to five times greater information capacity (Juusola and de Polavieja 2003; Juusola and Hardie 2001a). While the larger rhabdomere improves photon capture (Howard and Snyder 1983), other signal processing must complement this (van Hateren 1992). Accordingly, blowfly photoreceptors also have faster phototransduction reactions and membrane time constants (Weckström et al. 1991) than *Drosophila* photoreceptors (Juusola and Hardie 2001a) to prevent their responses from saturation.

Could LRLE photoreceptors have more phototransduction units than the other photoreceptors of this study? An increase in phototransduction units would increase the membrane area of photoreceptors and their effective capacitance. However, all the photoreceptors had similar membrane capacitances (Fig. 3, B and C), making it unlikely that LRLE photoreceptors would have more, larger, or denser microvilli. Although the voltage responses in LRLE photoreceptors are not faster than in LRDE photoreceptors (Fig. 2A), their speed surpasses that of DR photoreceptors. We therefore suggest that the higher information capacities of the LR photoreceptors over their DR counterparts stem from faster phototransduction reactions (cf. the broader signal bandwidths; Fig. 4), suitably matched with membrane properties (Fig. 3, B and C).

Studies of DR *Drosophila* (Juusola and Hardie 2001a,b) and hypomorphic *Drosophila* mutations of phospholipase C (PLC) and G protein (Pak et al. 1976; Scott and Zuker 1998; Scott et al. 1995) have attributed the bump timing (or latency distribution; cf. Wong et al. 1980) and waveform dynamics to two independent stages in the phototransduction cascade, whose convolution defines the photoreceptor response. The events determining the timing of the response are believed to occur largely at, or upstream of, PLC, whereas events determining the bump shape and amplitude are generated downstream of PLC and mediated by intracellular calcium. Because the bump latency distribution is generally much broader (i.e., the average timing lasts longer) than the average bump waveform (Juusola and Hardie 2001a), it both sets the speed limit for photoreceptor voltage responses and is a major factor in contrast gain (Juusola and Hardie 2001a,b). We therefore further suggest that light-rearing affects more of the early enzymatic reactions at, or upstream of, PLC than the later diffusion-bound membrane processes. Since the responses of LR photoreceptors were always faster than those of DR photoreceptors, some of the rearing-induced changes in the early phototransduction reactions are likely to be persistent. If true, this implies that the initial assembly of the phototransduction units during development would set the upper bound for future molecular permutations within these structures.

How do photoreceptor cells adjust to light exposure?

In contrast, the improvements in photoreceptor signaling caused by light exposure most probably reflect enhanced signal processing both down- and upstream of PLC. Attuned supply of phototransduction molecules together with attuned ion channel densities on the cell membrane could help to resist saturation (Figs. 2 and 4; cf. Niven et al. 2003; Weckström et al. 1991) and to reduce voltage noise (Figs. 4 and 5; cf. de Polavieja 2002; Stemmler and Koch 1999).

Previous works from our laboratory (Juusola and Hardie 2001a,b; Niven et al. 2003) have shown that, as *Drosophila* photoreceptors are light-adapted, the frequency response of the membrane, or the impedance function, speeds up in parallel with the phototransduction cascade so that at no point does it seriously compromise the bandwidth of the light current. Accordingly, if the improvements in the photoreceptors' signaling performance following the light exposure were caused by the translocations of phototransduction molecules and ion channels (cf. Böhner et al. 2002; Kiselev et al. 2000; Kosloff et al. 2003; Lee et al. 2003), we would expect these processes also to occur in parallel. Otherwise, the signaling would deteriorate: phototransduction signals would clip if the membrane low-passes too much (Juusola and Hardie 2001a) or they would be contaminated by high-frequency noise if filtered inadequately (van Hateren and Laughlin 1990).

The shared 2 h time-course of the molecular translocations (Böhner et al. 2002; Kiselev et al. 2000; Kosloff et al. 2003; Lee et al. 2003) and the reduction in the voltage noise (Fig. 4) allows us to link these findings. According to our hypothesis, since the maximum speed of phototransduction reactions is set by the rearing light conditions, the bandwidth of signaling can only broaden marginally (Fig. 5A). However, while the changes in the phototransduction reactions are bound to the changes in the ion channel compositions, the more precise phototransduction signals (Fig. 4) can be filtered by the correspondingly shifted membrane impedance. This improves the reliability of signaling within that bandwidth (Fig. 5A), allowing the information capacity of the DR photoreceptors to approach that of LR photoreceptors (Fig. 5B).

Differences in adaptation parameters

The protocol for WNC stimulation required photoreceptors to adapt to increasingly brighter background intensities. This background adaptation was accompanied by membrane potential depolarization, with an approximate steady-state established in about 30 s. Plotting the steady-state depolarization against the light background revealed that adaptation performed a logarithmic conversion of the light intensity (cf. Laughlin and Hardie 1978) whose scaling varied with the test regimens. Depolarization was less strong in LRLE photoreceptors (Fig. 6).

Another practical way to study adaptation to sustained light levels is to use shorter light pulses. Photoreceptors of our four test regimens responded to a 700-ms bright light pulse with the characteristic peak-to-plateau transitions of WT photoreceptors (Juusola and Hardie 2001a). Differences in trough amplitude, trough timing, and plateau depolarization could not be linked clearly to either rearing or exposure conditions (data not shown). However, the light pulse evoked oscillations in the plateau phase of responses. Although this is a novel finding in WT photoreceptors, it has been associated previously with two mutant phenotypes (Burg et al. 1996; Leung et al. 2000). Interestingly in WT photoreceptors, the incidence and the features of oscillations depended on rearing conditions.

Oscillations can have intracellular or interneural origins. They may result from a feedback in calcium-mediated photo-transduction reactions (Leung et al. 2000), a feedback from postsynaptic large monopolar cells (LMCs) to photoreceptor axons (Meinertzhagen and O'Neil 1991), or lateral interactions either between photoreceptor axons (van Hateren 1986) or neurons in the same neuro-ommatidia (Strausfeld 1976). However, whatever may be their cause, the oscillations could function to enhance synaptic signal transfer to LMCs. It has been shown in *Calliphora* that the voltage responses of large monopolar cells to light pulses often show detailed oscillations (van Hateren 1987). If the oscillations in LMCs are triggered and synchronized by transient stimulus patterns, the synaptic information transfer increases (Uusitalo et al. 1995). Therefore it is not implausible that, particularly in slow photoreceptors of DR flies, which showed oscillations most frequently, some homeostatic mechanism could be activated in the synapse to improve the transmission of fast signals.

Plasticity in higher-order visual centers

Our arguments about how parallel plastic changes may help to optimize the flow of information within photoreceptors can also be applied to the networks of visual neurons. Indeed, the preservation of constant neural images of objects in changing environments may require that the form and function of the whole visual system are tuned in line. Although different protocols used in different studies make it difficult to draw any clear conclusion about a common time-course behind the experience-dependent changes in *Drosophila* visual system, it is still worth to consider the wide range of findings reported so far. Modifications of visual behavior owing to experience-dependent plasticity in the visual system include associative changes in visual pattern and color preferences (Menne and Spatz 1977; Wolf and Heisenberg 1991). Rearing in different light conditions was also shown to affect visual orientation behavior (Hirsch et al. 1990) and locomotor activity (Martin et al. 1999). Furthermore, anatomical studies have indicated that light rearing increases the size of several parts of the visual processing pathways of *Drosophila*, including the lamina, mushroom bodies, and central complex (Barth 1997; Barth et al. 1997; Kral and Meinertzhagen 1989; Meinertzhagen 1989). Barth et al. (1997) argued that the growth in the lamina is most likely triggered by the light-evoked response of the photoreceptors. Finally, Hirsch and Tompkins (1994) and Hirsch et al. (1995) presented evidence that light conditions during rearing can affect the courtship behavior. These authors showed that females copulate faster with males that are reared in the same

light conditions, underlining the evolutionary significance of experience-dependent behavioral modifications (Barth et al. 1997).

ACKNOWLEDGMENTS

We thank G. Garcia de Polavieja, A. French, C. Huang, and H. Robinson for critical comments and J. Niven for help during the early stages of this study.

GRANTS

M. Juusola is supported by grants from the Royal Society, Biotechnology and Biological Sciences Research Council, and the Wellcome Trust. V. Wolfram is an Avrith Ph.D. Fellow.

REFERENCES

- Adrian RH and Almers W.** Membrane capacity measurements on frog skeletal muscle in media of low ion content. *J Physiol* 237: 573–605, 1974.
- Bähner M, Frechter S, Da Silva N, Minke B, Paulsen R, and Huber A.** Light-regulated subcellular translocation of *Drosophila* TRPL channels induces long-term adaptation and modifies the light-induced current. *Neuron* 34: 83–93, 2002.
- Barth M.** Vision affects mushroom bodies and central complex in *Drosophila melanogaster*. *Learn Mem* 4: 219–229, 1997.
- Barth M, Hirsch H, Meinertzhagen IA, and Heisenberg M.** Experience-dependent developmental plasticity in the optic lobe of *Drosophila melanogaster*. *J Neurosci* 17: 1493–1504, 1997.
- Bavelier D and Neville HJ.** Cross-modal plasticity: where and how? *Nat Rev Neurosci* 3: 443–452, 2002.
- Bear MF and Melenka RC.** Synaptic plasticity: LTP and LTD. *Curr Opin Neurobiol* 4: 389–399, 1994.
- Bendat JS and Piersol AG.** *Random Data: Analysis and Measurement Procedures*. New York: John Wiley, 1986.
- Brainard MS and Doupe AJ.** What songbirds teach us about learning. *Nature* 417: 351–358, 2002.
- Burg MG, Geng C, Guan Y, Koliantz G, and Pak WL.** *Drosophila* *rosA* gene, which when mutant causes aberrant photoreceptor oscillation, encodes a novel neurotransmitter transporter homologue. *J Neurogenet* 11: 59–79, 1996.
- Cover T and Thomas J.** *Elements of Information Theory*. New York: Wiley Interscience, 1991.
- Crair MC, Gillespie DC, and Stryker MP.** The role of visual experience in the development of columns in cat visual cortex. *Science* 279: 566–570, 1998.
- Davis GW and Goodman CS.** Genetic analysis of synaptic development and plasticity: homeostatic regulation of synaptic efficacy. *Curr Opin Neurobiol* 8: 149–156, 1998a.
- Davis GW and Goodman CS.** Synapse-specific control of synaptic efficacy at the terminals of a single neuron. *Nature* 392: 82–86, 1998b.
- Deimel E and Kral K.** Long-term sensitivity adjustment of the compound eyes of the housefly *Musca domestica* during early adult life. *J Insect Physiol* 38: 425–430, 1992.
- de Polavieja GG.** Errors drive the evolution of biological signalling to costly codes. *J Theor Biol* 214: 657–664, 2002.
- Desai NS, Cudmore RH, Nelson SB, and Turrigiano GG.** Critical periods for experience-dependent synaptic scaling in visual cortex. *Nat Neurosci* 5: 783–789, 2002.
- French AS, Holden AV, and Stein RB.** The estimation of the frequency response function of a mechanoreceptor. *Kybernetik* 11: 15–23, 1972.
- Goodman CS and Shatz CJ.** Developmental mechanisms that generate precise patterns of neuronal connectivity. *Cell* 72: 77–98, 1993.
- Hamdorf K.** The physiology of invertebrate visual pigments. In: *Handbook of Sensory Physiology* (vol. VII/6A), edited by Autrum H. Berlin: Springer-Verlag, 1979, p. 145–224.
- Hardie RC.** Functional organisation of the fly retina. *Prog Sens Physiol* 5: 1–79, 1985.
- Hardie RC.** Voltage-sensitive potassium channels in *Drosophila* photoreceptors. *J Neurosci* 11: 3079–3095, 1991a.
- Hardie RC.** Whole-cell recordings of the light-induced current in dissociated *drosophila* photoreceptors—evidence for feedback by calcium permeating the light-sensitive channels. *Proc R Soc Lond B Biol Sci* 245: 203–210, 1991b.
- Hardie RC and Raghu P.** Visual transduction in *Drosophila*. *Nature* 413: 186–193, 2001.

- Henderson SR, Reuss H, and Hardie RC.** Single photon responses in *Drosophila* photoreceptors and their regulation by Ca^{2+} . *J Physiol* 524: 79–94, 2000.
- Hertel H.** The effect of spectral light deprivation on the spectral sensitivity of the honeybee. *J Comp Physiol [A]* 147: 365–369, 1982.
- Hertel H.** Change of synapse frequency in certain photoreceptors of the honeybee after chromatic deprivation. *J Comp Physiol [A]* 151: 477–482, 1983.
- Hirsch HV and Tompkins L.** The flexible fly: experience-dependent development of complex behaviors in *Drosophila melanogaster*. *J Exp Biol* 195: 1–18, 1994.
- Hirsch HV, Barth M, Luo S, Sambaziotis H, Huber M, Possidente D, Ghiradella H, and Tompkins L.** Early visual experience affects mate choice of *Drosophila melanogaster*. *Anim Behav* 50: 1211–1217, 1995.
- Hirsch HV, Potter D, Zawierucha D, Choudhri T, Glasser A, Murphey RK, and Byers D.** Rearing in darkness changes visually-guided choice behavior in *Drosophila*. *Vis Neurosci* 5: 281–289, 1990.
- Howard J and Snyder AW.** Transduction as a limitation on compound eye function and design. *Proc R Soc Lond B Biol Sci* 217: 287–307, 1983.
- Howard J, Blakeslee B, and Laughlin SB.** The intracellular pupil mechanism and the maintenance of photoreceptor signal to noise ratios in the blowfly *Lucilia cuprina*. *Proc R Soc Lond B Biol Sci* 23: 415–435, 1987.
- Hubel DH and Wiesel TN.** The period of susceptibility to the physiological effects of unilateral eye closure in kittens. *J Physiol* 206: 419–436, 1970.
- Hubel DH, Wiesel TN, and LeVay S.** Plasticity of ocular dominance columns in monkey striate cortex. *Philos Trans R Soc Lond B Biol Sci* 278: 377–409, 1977.
- Juusola M.** Linear and nonlinear contrast coding in light-adapted blowfly photoreceptors. *J Comp Physiol [A]* 172: 511–521, 1993.
- Juusola M and de Polavieja GG.** The rate of information transfer of naturalistic stimulation by graded potentials. *J Gen Physiol* 122: 191–206, 2003.
- Juusola M and French AS.** The efficiency of sensory information coding by mechanoreceptor neurons. *Neuron* 18: 959–968, 1997.
- Juusola M and Hardie RC.** Light adaptation in *Drosophila* photoreceptors. I. Response dynamics and signaling efficiency at 25°C. *J Gen Physiol* 117: 3–25, 2001a.
- Juusola M and Hardie RC.** Light adaptation in *Drosophila* photoreceptors. II. Rising temperature increases the bandwidth of reliable signaling. *J Gen Physiol* 117: 27–42, 2001b.
- Juusola M and Weckström M.** Band-pass filtering by voltage-dependent membrane in an insect photoreceptor. *J Neurosci Lett* 154: 84–88, 1993.
- Juusola M, Kouvalainen E, Järvillehto M, and Weckström M.** Contrast gain, signal-to-noise ratio and linearity in light-adapted blowfly photoreceptors. *J Gen Physiol* 104: 593–621, 1994.
- Juusola M, Niven JE, and French AS.** Shaker K^+ channels contribute early nonlinear amplification to the light response in *Drosophila* photoreceptors. *J Neurophysiol* 90: 2014–2021, 2003.
- Katz LC and Shatz CJ.** Synaptic activity and the construction of cortical circuits. *Science* 274: 1133–1138, 1996.
- Kiselev A, Socolich M, Vinos J, Hardy RW, Zuker CS, and Ranganathan R.** A molecular pathway for light-dependent photoreceptor apoptosis in *Drosophila*. *Neuron* 28: 139–152, 2000.
- Knudsen EI and Brainard MS.** Visual instruction of the neural map of auditory space in the developing optic tectum. *Science* 253: 85–87, 1991.
- Kosloff M, Elia N, Joel-Almagor T, Timberg R, Zars TD, Hyde DR, Minke B, and Selinger Z.** Regulation of light-dependent Gqalpha translocation and morphological changes in fly photoreceptors. *EMBO J* 22: 459–468, 2003.
- Kouvalainen E, Weckström M, and Juusola M.** Determination of signal-to-noise ratio and linearity in light-adapted blowfly photoreceptors. *Vis Neurosci* 95: 1221–1225, 1994.
- Kral K and Meinertzhagen IA.** Anatomical plasticity of synapses in the lamina of the optic lobe of the fly. *Philos Trans R Soc Lond B Biol Sci* 323: 155–183, 1989.
- Laughlin SB.** The role of sensory adaptation in the retina. *J Exp Biol* 146: 39–62, 1989.
- Laughlin SB and Hardie RC.** Common strategies for light adaptation in the peripheral visual systems of fly and dragonfly. *J Comp Physiol [A]* 128: 319–340, 1978.
- Lee SJ, Xu H, Kang LW, Amzel LM, and Montell C.** Light adaptation through phosphoinositide-regulated translocation of *Drosophila* visual arrestin. *Neuron* 39: 121–132, 2003.
- Leung HT, Geng C, and Pak WL.** Phenotypes of *trpl* mutants and interactions between the transient receptor potential (TRP) and TRP-like channels in *Drosophila*. *J Neurosci* 20: 6797–6803, 2000.
- Marmarelis PZ and Marmarelis VZ.** *Analysis of Physiological Systems: The White Noise Approach*. New York: Plenum Publishing, 1978.
- Martin JR, Ernst R, and Heisenberg M.** Temporal pattern of locomotor activity in *Drosophila melanogaster*. *J Comp Physiol [A]* 184: 73–84, 1999.
- Meinertzhagen IA.** Fly photoreceptor synapses—their development, evolution, and plasticity. *J Neurobiol* 20: 276–294, 1989.
- Meinertzhagen IA and O’Neil SD.** Synaptic organization of columnar elements in the lamina of the wild type in *Drosophila melanogaster*. *J Comp Neurol* 305: 232–263, 1991.
- Menne D and Spatz HC.** Colour vision in *Drosophila melanogaster*. *J Comp Physiol [A]* 114: 301–312, 1977.
- Mimura K.** Development of visual pattern discrimination on the fly depends on light experience. *Science* 232: 83–85, 1986.
- Mooney R.** Sensitive periods and circuits for learned birdsong. *Curr Opin Neurobiol* 9: 121–127, 1999.
- Niven JE, Vahasoyrinki M, Kauranen M, Hardie RC, Juusola M, and Weckström M.** The contribution of Shaker K^+ channels to the information capacity of *Drosophila* photoreceptors. *Nature* 421: 630–634, 2003.
- Pak WL, Ostroy SE, Deland MC, and Wu C-F.** Photoreceptor mutant of *Drosophila*: is protein involved in intermediate steps of phototransduction? *Science* 194: 956–959, 1976.
- Palleroni A and Hauser M.** Experience-dependent plasticity for auditory processing in a raptor. *Science* 299: 1195, 2003.
- Payne R and Howard J.** Response of an insect photoreceptor: a simple log-normal model. *Nature* 290: 415–416, 1981.
- Schneider MF and Chandler WK.** Effects of membrane potential on the capacitance of skeletal muscle fibers. *J Gen Physiol* 67: 125–163, 1976.
- Scott K and Zuker CS.** Assembly of the *Drosophila* phototransduction cascade into a signalling complex shapes elementary responses. *Nature* 395: 805–808, 1998.
- Scott K, Becker A, Sun Y, Hardy R, and Zuker CS.** G(alpha) protein function in vivo: genetic dissection of its role in photoreceptor cell physiology. *Neuron* 15: 919–927, 1995.
- Shannon CE.** A mathematical theory of communication. *Bell Syst Tech J* 27: 379–423, 1948.
- Spekreijse H and Oostings H.** Linearizing: a method for analysing and synthesizing non-linear systems. *Kybernetik* 7: 20–30, 1970.
- Spekreijse H and van der Tweel LH.** Linearization of evoked responses to sine wave-modulated light by noise. *Nature* 205: 913, 1965.
- Stemmler M and Koch C.** How voltage-dependent conductances can adapt to maximize the information encoded by neuronal firing rate. *Nat Neurosci* 2: 521–527, 1999.
- Strausfeld NJ.** *Atlas of an Insect Brain*. Berlin: Springer-Verlag, 1976.
- Suster ML and Bate M.** Embryonic assembly of a central pattern generator without sensory input. *Nature* 416: 174–178, 2002.
- Turrigiano GG.** Homeostatic plasticity in neuronal networks: the more things change, the more they stay the same. *Trends Neurosci* 22: 221–227, 1999.
- Uusitalo RO, Juusola M, and Weckström M.** Graded responses and spiking properties of identified first-order visual interneurons of the fly compound eye. *J Neurophysiol* 73: 1782–1792, 1995.
- van Hateren JH.** Electrical coupling of neuro-ommatidial photoreceptor cells in the blowfly. *J Comp Physiol [A]* 158: 795–811, 1986.
- van Hateren JH.** Neural superposition and oscillations in the eye of the blowfly. *J Comp Physiol [A]* 161: 849–855, 1987.
- van Hateren JH.** Theoretical predictions of spatiotemporal receptive fields of fly LMCs, and experimental validation. *J Comp Physiol [A]* 171: 157–170, 1992.
- van Hateren JH and Laughlin SB.** Membrane parameters, signal transmission, and the design of a graded potential neuron. *J Comp Physiol [A]* 166: 437–448, 1990.
- Weckström M and Laughlin SB.** Visual ecology and voltage-gated ion channels in insect photoreceptors. *Trends Neurosci* 18: 17–21, 1995.
- Weckström M, Hardie RC, and Laughlin SB.** Voltage-activated potassium channels in blowfly photoreceptors and their role in light adaptation. *J Physiol* 440: 635–657, 1991.
- Wolf R and Heisenberg M.** Basic organization of operant behaviour as revealed in *Drosophila* flight orientation. *J Comp Physiol [A]* 169: 699–707, 1991.
- Wong F, Knight BW, and Dodge FA.** Dispersion of latencies in photoreceptors of *Limulus* and the adapting-bump model. *J Gen Physiol* 76: 517–537, 1980.